Neurobiology of Disease 190 (2024) 106385

Contents lists available at ScienceDirect

Neurobiology of Disease

journal homepage: www.elsevier.com/locate/ynbdi

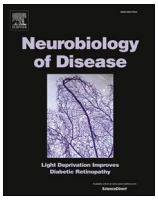

Midlife insulin resistance, *APOE* genotype, and change in late-life brain beta-amyloid accumulation – A 5-year follow-up [^{11}C]PIB-PET study

Elina Pietilä [a,*], Anniina Snellman [a], Jouni Tuisku [a], Semi Helin [a], Matti Viitanen [b,c], Antti Jula [d], Juha O. Rinne [a,e], Laura L. Ekblad [a,f]

[a] *Turku PET Centre, University of Turku and Turku University Hospital, Turku, Finland*
[b] *Department of Geriatrics, Turku City Hospital and University of Turku, Finland*
[c] *Division of Clinical Geriatrics, NVS, Karolinska Institutet, Stockholm, Sweden*
[d] *Finnish Institute for Health and Welfare, Turku, Finland*
[e] *InFLAMES Reseach Flagship Center, University of Turku, Turku, Finland*
[f] *Department of Geriatrics, Turku University Hospital, Wellbeing services county of Southwestern Finland, Finland*

ARTICLE INFO

Keywords:
Insulin resistance
HOMA-IR
APOEe4
[11C]PIB-PET
Beta-amyloid
Alzheimer's disease

ABSTRACT

We studied if midlife insulin resistance (IR) and *APOE* genotype would predict brain beta-amyloid (Aβ) accumulation and Aβ change in late-life in 5-year follow-up [^{11}C]PIB-PET study. 43 dementia-free participants were scanned twice with [^{11}C]PIB-PET in their late-life (mean age at follow-up 75.4 years). Participants were recruited from the Finnish Health2000 study according to their HOMA-IR values measured in midlife (mean age at midlife 55.4 years; IR+ group, HOMA-IR > 2.17; IR− group, HOMA-IR <1.25), and their *APOE*ε4 genotype. At late-life follow-up, [^{11}C]PIB-PET composite SUVr was significantly higher in IR+ group than IR− group (median 2.3 (interquartile range 1.7–3.3) vs. 1.7 (1.5–2.4), $p = 0.03$). There was no difference between IR- and IR+ groups in [^{11}C]PIB-PET SUVr 5-year change, but the change was significantly higher in IR+/*APOE*ε4+ group (median change 0.8 (0.60–1.0)) than in IR−/*APOE*ε4− (0.28 (0.14–0.47), $p = 0.02$) and in IR+/*APOE*ε4− group (0.24 (0.06–0.40), $p = 0.046$). These results suggest that *APOE*ε4 carriers with midlife IR are at increased risk for late-life Aβ accumulation.

1. Introduction

Metabolic risk factors, such as insulin resistance (IR) (Ekblad et al., 2017; Peila et al., 2002), obesity (Kivipelto et al., 2005; Tang et al., 2021) and type 2 diabetes (Chatterjee et al., 2016) have been shown to associate with cognitive decline and dementia. Previous research indicates there to be an association between IR and brain amyloid-beta (Aβ) accumulation (Ekblad et al., 2018), which is considered to be the earliest pathological hallmark of Alzheimer's disease (AD). While the neurobiological mechanisms of this association have not yet been fully elucidated (Shieh et al., 2020), the brain has been found to be insulin resistant in AD even in the absence of diabetes (Talbot et al., 2012; Kim and Arvanitakis, 2023; Leclerc et al., 2022; Molina-Fernández et al., 2022). Thus, it is reasonable to believe that IR might be associated with subsequent amyloid accumulation or dementia.

There is a paucity of research focusing on the association between midlife insulin resistance and brain Aβ accumulation in cognitively healthy people. The existing studies are methodologically heterogenous and the findings have been mixed: Some prospective studies have linked various measures of metabolic risk factors, such as HOMA-IR (Ekblad et al., 2018), elevated BMI (Gottesman et al., 2017), dyslipidemia (Vemuri and Schöll, 2017) and diabetes (van Arendonk et al., 2023) at late-midlife to brain Aβ accumulation. Furthermore, findings from a cross-sectional study indicated HOMA-IR status to be associated with higher Aβ burden in frontal and temporal brain areas (Willette et al., 2015). However, there are longitudinal studies that have not found an association between midlife insulin resistance and Aβ accumulation in late-life, measured with 2 h OGTT and HOMA-IR (Thambisetty et al.,

Abbreviations: [^{11}C]PIB-PET, Pittsburgh compound B PET; Aβ, beta-amyloid; AD, Alzheimer disease; BMI, body mass index; BP, blood pressure; CERAD, Consortium to Establish a Registry for Alzheimer's Disease; HOMA-IR, homeostatic model assessment of insulin resistance; IR, insulin resistance; OGTT, Oral glucose tolerance tests; PET, positron emission tomography; ROI, region of interest; SUVr, standardized uptake value ratio.

* Corresponding author.
E-mail address: empiet@utu.fi (E. Pietilä).

https://doi.org/10.1016/j.nbd.2023.106385
Received 5 October 2023; Received in revised form 14 December 2023; Accepted 14 December 2023
Available online 18 December 2023

2013), and neither with midlife diabetes (Gottesman et al., 2017; Vemuri and Schöll, 2017; van Arendonk et al., 2023) nor obesity (Vemuri and Schöll, 2017; van Arendonk et al., 2023). Hence, further research with prospective data is clearly needed to explore this association.

We have previously found that midlife IR was independently associated with brain Aβ accumulation in elderly individuals without dementia (Ekblad et al., 2018). In the present study we have extended the follow-up by five years and provide repeated measurements of brain Aβ burden using [^{11}C]PIB-PET. We hypothesized that IR measured with HOMA-IR in midlife would predict higher brain Aβ burden 20 years later and a greater increase in brain Aβ accumulation during the 5-year imaging follow-up from 15 to 20 years after the measurement of midlife HOMA-IR. It is well-established that *APOE*ε4 genotype is an important risk factor for Aβ accumulation (Jansen et al., 2022). *APOE*ε4 genotype is also associated with vascular risk factors (Lumsden et al., 2020) which in turn, often associate with insulin resistance and are also associated with cognitive decline. Therefore, our secondary hypothesis was that *APOE* genotype might modulate the association between IR and Aβ accumulation. To test these hypotheses, we re-examined 43 elderly volunteers after approximately 5 years with [^{11}C]PIB-PET and analyzed differences between IR groups in Aβ load at the late-life follow-up and the change in Aβ accumulation during the 5-year follow-up. Secondary analyses were performed in groups stratified according to *APOE*ε4 genotype.

2. Methods

This longitudinal neuroimaging study population included 43 participants. The participants were originally recruited from the Finnish population-based Health 2000 study (Heistaro, 2008) according to their homeostatic model assessment of insulin resistance (HOMA-IR) values measured in their midlife in 2000, and *APOE*ε4 genotype. [11C]PIB-PET imaging was conducted twice with [11C]PIB-PET in their late-life. Here we report the results from the late-life 5-year follow-up [11C]PIB-PET study.

2.1. Health 2000 study

The Health 2000 survey is a Finnish nationwide, population-based study by the Finnish Institute for Health and Welfare with baseline data collection in the years 2000–2001. The study population was a representative sample of the Finnish adult population. 8028 individuals aged 30 years or over were selected randomly from the Finnish population register. 6354 of them (79% participation rate, mean age 55.4 years) participated in the health examination proper. A thorough health examination was conducted, and venous blood samples were collected (Heistaro, 2008). *APOE* genotype was defined with the MassARRAY System (Sequenom, San Diego, CA, USA) with a modified protocol (Jänis et al., 2004). The recruitment processes of the Health 2000 survey (Heistaro, 2008) have been described in detail previously.

2.2. Study population and recruitment

The study recruitment process is represented in Fig. 1. In late-life baseline in 2014, 60 dementia-free participants were recruited from those who had attended the Health 2000 survey according their HOMA-IR in their midlife in the year 2000 and *APOE*ε4 genotype. The size of the study was based on power calculations of test–retest analyses of [^{11}C]PIB-PET scans, which indicated that for a 90% power to obtain a statistically significant difference between groups, 5 persons per group would be needed to detect a 15% difference in Aβ accumulation in the frontal cortex (Aalto et al., 2009). Two groups were formed: The insulin resistance group (IR+, HOMA-IR > 2.17 in the year 2000, highest tertile of the Health 2000 study population) and the control group (IR−, HOMA-IR <1.25 in the year 2000, lowest tertile of the Health 2000 study population). Both groups included 30 participants and 50% *APOE*ε4 carriers. Because *APOE*ε4 genotype is a strong risk factor for Aβ accumulation, the study was designed to include an equal number of *APOE*ε4 carriers in both groups. The recruitment processes of the late-life baseline[^{11}*C*]PIB-PET study have been described in detail previously (Ekblad et al., 2018). The results of the 2014–2016 late-life baseline [^{11}C]PIB-PET study have been published previously (Ekblad et al., 2018; Toppala et al., 2021; Toppala et al., 2019).

Late-life follow-up [^{11}C]PIB-PET imaging study was conducted in the years 2019–2021. All the 60 participants who had taken part in our multimodal imaging study in late-life baseline were invited to participate in the re-examinations after 5 years in late-life follow-up study. Participants were invited with a recruitment letter sent via the Finnish Institute for Health and Welfare. Altogether 55 individuals responded to the letter; two people did not respond; and three people had died during the follow-up. For data protection issues the Institute of Health and Welfare did not provide data on causes of these deaths. 46 were willing to participate; nine refused. Of those willing to participate three individuals were further excluded from PET imaging due to miscellaneous reasons (did not want to undergo PET imaging (1); could not undergo MRI imaging (1); was diagnosed with AD before PET imaging (1)). Consequently, 43 elderly individuals took part in the 5-year late-life follow-up and were included in the analyses of the present study.

Exclusion criteria for the late-life baseline study were type 2 diabetes in midlife, history of major stroke, any major neurological disease, diagnosis of dementia, and a contraindication for PET or MRI scan and, for the IR− group, diagnosis of type 2 diabetes after the year 2000. Those with both a risk allele and a protective allele for AD (ε4/ε2) were not included.

2.3. Laboratory assessments

The methods of laboratory assessment in midlife in the year 2000 have been previously described (Toppala et al., 2019). HOMA-IR was calculated by the following equation: fasting insulin (μU/mL) × fasting glucose (mmol/L)/22.5 (Matthews et al., 1985). The methods of laboratory assessments in late-life baseline study in 2014–2016 have been described in previous publications (Ekblad et al., 2018; Toppala et al., 2019). At the follow-up in 2019–2021 insulin was determined by ECLIA (electrochemiluminescence immunoassay) with a Cobas e801 immunochemistry analyzer (Roche Diagnostics GmbH, Mannheim, Germany), glucose by enzymatic photometry with a Cobas c702 chemistry analyzer (Roche Diagnostics GmbH), and hemoglobin A_{1c} with an immunochemical method with a Cobas c501 and c513 analyzers (Roche Diagnostics GmbH). Venous blood samples were drawn after an overnight fast (minimum 10 h).

2.4. Study protocol

PET and magnetic resonance imaging (MRI) was conducted at the Turku PET Centre. The participants underwent MRI with a 3-T MRI scanner (Philips Ingenuity TF PET-MR device, Philips Healthcare, Amsterdam, the Netherlands) to obtain anatomic reference and to exclude possible structural abnormalities. The same scanner and the same scanning protocol was used at both time points.

[^{11}C]PIB-PET imaging was performed to assess Aβ burden in the brain. A brain-dedicated high-resolution PET scanner, the ECAT HRRT (Siemens Medical Solutions, Knoxville, TN) was used at both time points. An individually shaped thermoplastic mask was used to minimize head movement. An external position detector (Polaris Vicra; Northern Digital, Waterloo, Canada) was used to monitor possible movements of the head. [^{11}C]PIB was manufactured as previously reported (Snellman et al., 2017). The PET-scanning protocol at baseline in 2014–2016 has been described previously (Ekblad et al., 2018). In 2014–2016 [^{11}C]PIB-PET was performed as a dynamic 90-min scan. In 2019–2021 a shorter study protocol was used for better compliance. A

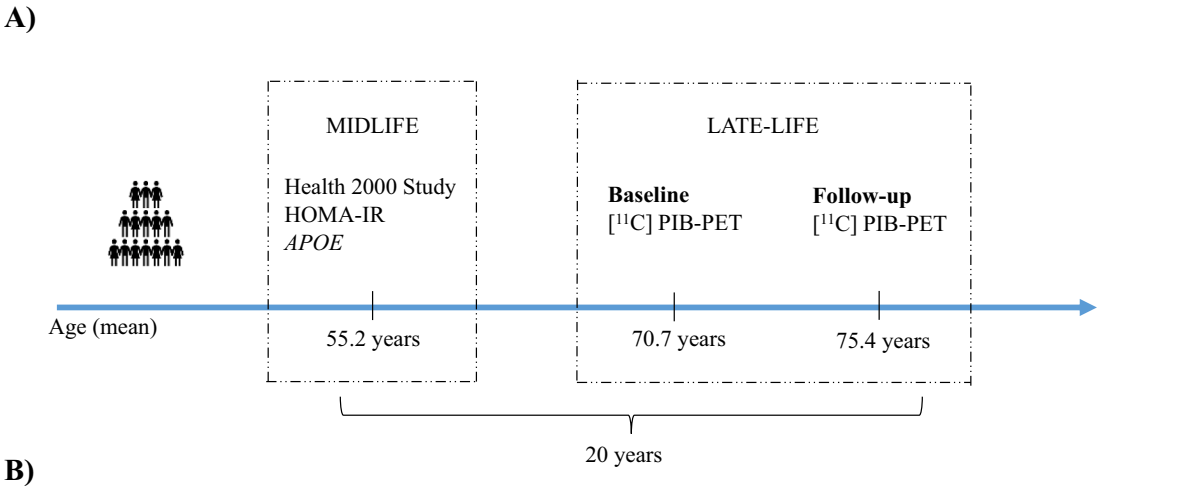

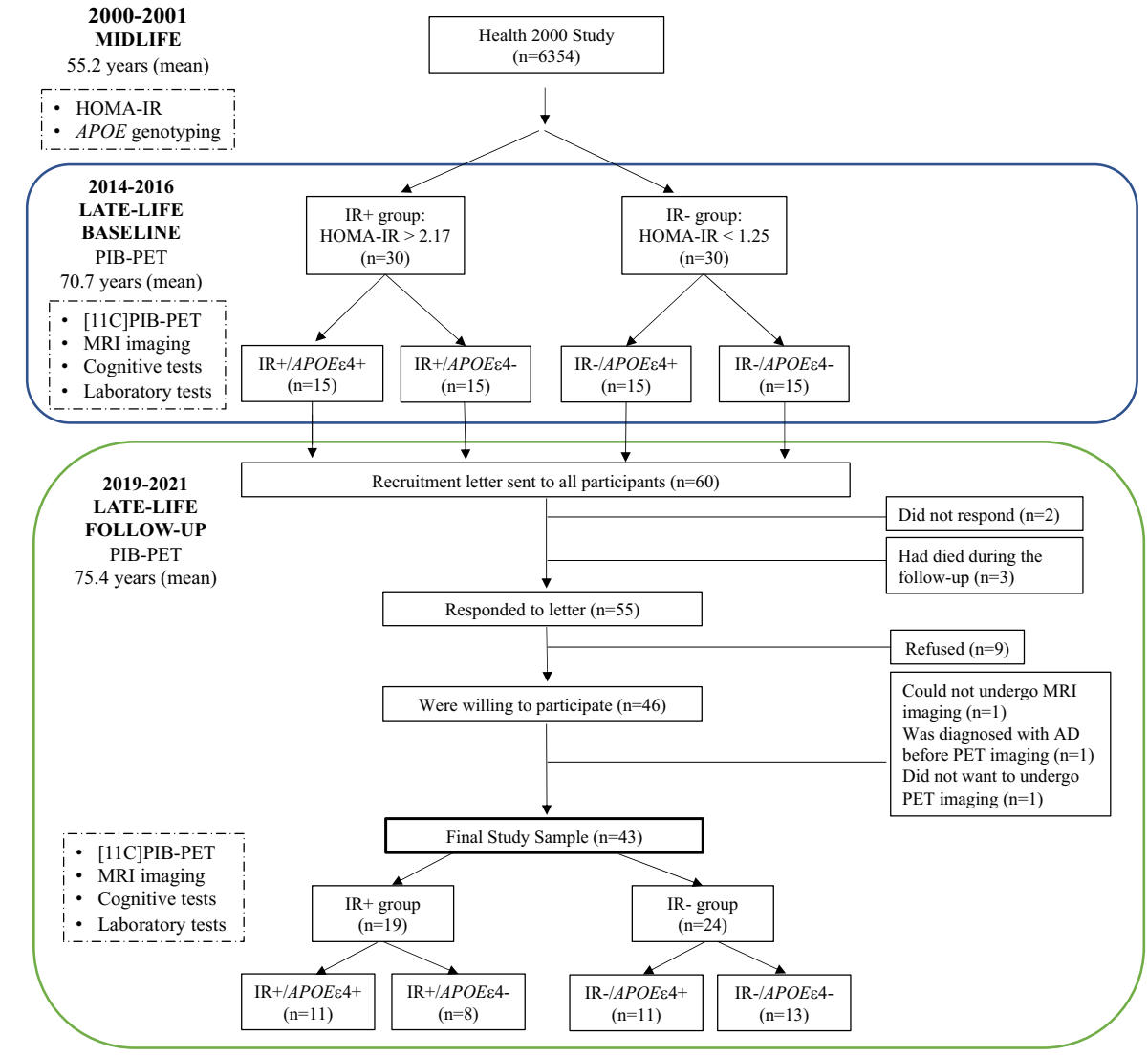

Fig. 1. Time line and flow chart of the study population.
The participants of the present [^{11}C]PIB-PET imaging study were recruited from the Health 2000 Study population according to the homeostatic model assessment of insulin resistance (HOMA-IR) values measured in their midlife and their *APOE* genotype. The late-life examinations included [11C]PIB-PET imaging at approximately 15 and 20 years after the midlife measurements. Mean age at each time point is shown for the present study population (n = 43) (A). A flow-chart of the study recruitment process and of those who dropped out from the late-life follow-up study (B).

mean dose of 491 MBq (SD 24) [^{11}C]PIB was administered intravenously outside the PET camera. The participants were instructed to lie down for 30 min before being positioned inside the scanner. The PET scan was started at 40 min from injection and the scan time was 50 min (40 to 90 min).

2.5. Brain PET data analysis with Magia toolbox

All the late-life PET data were analyzed using an in-house Magia toolbox pipeline (Karjalainen et al., 2020). The Magia toolbox is a standardized and fully automatic analysis pipeline for reproducible processing and kinetic modelling of brain PET data, running on MATLAB (The MathWorks, Inc., Natick, MA, USA), and including brain image preprocessing methods from SPM12-toolbox (Statistical Parametric Mapping; Wellcome Trust Centre for Neuroimaging, London, UK) and FreeSurfer (version 6.3, http://freesurfer.net/). Since the Magia toolbox was not used in our previous work (Ekblad et al., 2018), the PET data from the late-life baseline study was re-processed for the present study. Using Magia, all PET images were first motion-corrected and then co-registrated with the T1 MRI. Next, the pipeline produced voxel-by-voxel [^{11}C]PIB standardized uptake value ratio (SUVr) images by utilizing imaging data from 60 to 90 min after tracer injection. For the main outcome, a composite cortical [^{11}C]PIB score was calculated as a volume-weighted average of regions of interest (ROI) by using FreeSurfer anatomical parcellations. ROIs were based on regions where Aβ accumulation typically appears first in AD (Grothe et al., 2017) (parietal

Table 1
Characteristics of the study population according to A) insulin resistance (IR) groups and B) according to insulin resistance and *APOE* genotype at different phases of the study.

A)	IR-	IR+	*p* value
Midlife Health 2000 Study in 2000			
N (n/%)	24 (56%)	19 (44%)	
Women (n/%)	14 (58%)	9 (47%)	0.47
Age (years)	54.5 (52.3–56)	55 (53–57)	0.51
HOMA-IR 2000	0.9 (0.2)	3.3 (0.9)	<0.0001
APOE ε4 genotype (n/%)	11 (46%)	11 (58%)	0.43
Education (years)	12.5 (10.3–16.8)	9 (8–15)	0.03
Late-life baseline PIB-PET scan in 2014–2016			
Age at time PET scan (years)	70.5 (3.7)	71.0 (3.0)	0.56
HOMA-IR	1.8 (1.0)	5.4 (4.5)	<0.0001
BMI (kg/m^2)	24.4 (2.6)	29.5 (4.2)	0.0001
HbA1c (mmol/mol), mean (SD)	34.4 (3.6)	38.2 (6.9)	0.03
Serum total cholesterol (mmol/l)	5.3 (1.1)	4.9 (0.8)	0.3
Medication for T2DM (n(%))	0 (0%)	5 (26%)	0.008
CERAD total score	92 (87.5–95)	86 (75–91)	0.014
Late-life follow-up PIB-PET scan in 2019–2021			
Age at time PET scan (years)	74.1 (72.5–77.0)	74.8 (73.4–77.1)	0.50
Time between PET scans (years)	4.8 (0.6)	4.5 (0.7)	0.13
Time from Health 2000 (years)	20.3 (0.7)	20.2 (0.5)	0.67
HOMA-IR	1.9 (1.1)	4.6 (2.7)	<0.0001
BMI (kg/m^2)	25.6 (22.3–27.2)	28.9 (26.0–34.4)	0.002
HbA1c (mmol/mol)	37.5 (3.4)	41.7 (5.7)	0.008
Serum total cholesterol (mmol/l)	5.11 (1.0)	4.2 (0.9)	0.004
Medication for T2DM (n(%))	0 (0%)	6 (32%)	0.003
[^{11}C]PIB dose (MBq)	490 (476–503)	501 (489–505)	0.11
CERAD total score	90 (82.3–93)	78 (71–82)	0.0002

B)	IR-/APOEε4-	IR+/APOEε4-	IR-/APOEε4+	IR+/APOEε4+	*p* value
Late-life follow-up PIB-PET scan in 2019–2021					
N	13	8	11	11	
Women (n/%)	6/46%	4/50%	8/72%	5/45%	0.52
Age at late-life baseline PET scan (years)	71.0 (4.4)	71.1 (4.3)	69.9 (2.8)	71.0 (1.9)	0.82
Age at time late-life follow-up PET scan (years)	73.8 (72.6–78.8)	75.1 (72.0–79.4)	74.8 (72.3–77.2)	74.8 (73.8–77.1)	0.84
Time between PET scans (years)	5.0 (0.7)	4.7 (0.3)	4.7 (0.3)	4.5 (0.8)	0.44
HOMA-IR	1.9 (1.0)	5.6 (2.7)	1.9 (1.1)	3.8 (2.6)	0.0002
BMI (kg/m^2)	25.9 (22.6–28.2)	34.5 (30.2–36.2)	25.4 (22.1–27.2)	27.0 (24.2–28.9)	0.0013
HbA1c (mmol/mol)	38.7 (3.3)	44.0 (6.0)	36.1 (2.9)	40.1 (5.1)	0.0034
Serum total cholesterol (mmol/l)	4.9 (0.9)	4.3 (0.9)	5.4 (1.2)	4.1 (0.9)	0.025
Medication for T2DM (n/%)	0/0%	5/63%	0/0%	1/9%	0.0002
Education (years)	13 (10.5–17.5)	9 (8–11)	12 (10–15)	9 (8–18)	0.08
CERAD total score 2014–2016	92 (90–96)	88 (77–94)	91 (87–95)	83 (72–90)	0.07
CERAD total score 2019–2021	90 (83–93)	78 (68–84)	89 (82–93)	79 (72–81)	0.0024

Study population characteristics according to (A) insulin resistance (IR) groups, and (B) IR and *APOE* genotype groups. IR was defined by Homeostatic Model Assessment for Insulin Resistance (HOMA-IR) values in participants' midlife from the Health 2000 Study.
Differences between the IR groups were assessed with Two Sample t-test for normally distributed variables; with the Wilcoxon Rank sum test for variables with a skewed distribution (CERAD total scores, [^{11}C]PIB dose, education, body mass index (BMI) at follow-up, and age in 2000 and 2019–2021); and with Pearson's Chi-Square test for categorical variables. A logarithmic transformation was used for HOMA-IR at all time points, and HbA1c (hemoglobin A1c) and age at baseline to achieve normal distribution. Differences between the IR/APOE groups were assessed with one-way ANOVA and Kruskal-Wallis test. The results are shown as mean (SD) or median (interquartile range) unless stated otherwise. *p*-value indicates overall differences between groups.

cortex, prefrontal cortex, anterior cingulum, posterior cingulum, precuneus, lateral temporal cortex). The exact FreeSurfer regions for each ROI have been described in our previous article (Toppala et al., 2021). Cerebellar cortex was utilized as a reference region (Lopresti et al., 2005).

The change in [^{11}C]PIB composite score from late-life baseline to follow-up was calculated as [^{11}C]PIB composite score at late-life follow-up in 2019–2021 subtracted by [^{11}C]PIB composite score at late-life baseline in 2014–2016. Additionally, the [^{11}C]PIB SUVr images were spatially normalized and smoothed with 3D Gaussian 8 mm FWHM (Full Width at Half Maximum) filter, in order to carry out voxel level analyses.

2.6. Cognitive tests and demographic variables

Cognitive testing was performed at follow-up by trained psychology students according to the Finnish version of the Consortium to Establish a Registry for Alzheimer's Disease (CERAD) test (Morris et al., 1989) and CERAD total score was counted as previously reported (Chandler et al., 2005). Level of education was defined as years by interview.

2.7. Standard protocol approvals, registrations, and patient consents

The Finnish Health 2000 study was approved by the Ethics Committee for Epidemiology and Public Health in the hospital district of Helsinki and Uusimaa, Finland. The late-life baseline and follow-up [^{11}C]PIB-PET imaging studies were approved by the Ethics Committee of the Hospital District of Southwest Finland. All participants gave written informed consent before they attended the studies. All study procedures were conducted according to Good Clinical Practice guidelines and the Declaration of Helsinki.

2.8. Statistical analysis

To analyze the differences between IR− and IR+ groups in study characteristics we used Student's two-sample *t*-test for variables with a normal distribution, the Wilcoxon rank sum test for variables with a skewed distribution, and Pearson's ChiSquare test for categorical variables (Table 1A.). Differences in characteristics among the IR groups further stratified by *APOE*ε4 genotype were analyzed with ANOVA or Kruskall-Wallis test, and post-hoc pairwise differences between each IR/*APOE* group were assessed with Tukey's honest significant test or with the Steel-Dwass method (Table 1B.) A logarithmic transformation was used for HOMA-IR at all time points, and HbA1c (hemoglobin A1c) and age at baseline to achieve normal distribution. Differences between the 17 individuals who did not attend the follow-up analyses and those who attended were evaluated with Wilcoxon test/ Pearson's ChiSquare test.

Differences in [^{11}C]PIB composite SUVr at follow-up between the IR groups was compared with Wilcoxon rank sum test and among the further stratified IR/*APOE*ε4 groups with Kruskall-Wallis test, followed by pair-wise comparisons with the Steel-Dwass method. Differences in the change in [^{11}C]PIB composite SUVr during the 5-year follow-up were analyzed similarly.

The interaction of 'IR group × *APOE*ε4 genotype' on the association with [^{11}C]PIB composite SUVr at follow-up and the change in [^{11}C]PIB composite SUVr during the 5-year follow-up was evaluated with linear models where IR group, *APOE*ε4 genotype and the interaction term were entered as predictors.

To evaluate if *APOE* genotype, age, sex or education would impact the results considering IR group differences in [^{11}C]PIB composite SUVr at follow-up or the change in [^{11}C]PIB composite SUVr during the 5-year follow-up we also ran linear models adjusted for *APOE* genotype, and *APOE* genotype, age, sex and education. In addition, analyses for differences in the change in [^{11}C]PIB composite SUVr during the 5-year follow-up were further adjusted for time from baseline to follow-up. The normality assumption of these linear models was inspected from the residuals.

Spearman's correlation was utilized to assess the association between continuous HOMA-IR and Aβ accumulation.

Voxel-wise analyses for the differences in the change in [^{11}C]PIB composite SUVr during the 5-year follow-up between the "highest risk" i.e. IR+/ *APOE*ε4+ and the "lowest risk", IR−/ *APOE*ε4− groups without pre-defined ROIs were carried out in SPM12 for demonstrative purposes. First, normalized and smoothed delta SUVr maps were obtained by calculating the difference of normalized and smoothed follow-up and baseline [^{11}C]PIB SUVr images. Then, differences in these delta SUVr images between the IR+/ *APOE*ε4+ and IR−/ *APOE*ε4− groups were evaluated with two-sample *t*-test, combining p-value <0.0001 with cluster-level false discovery rate (FDR) correction ($p < 0.05$) for multiple comparisons.

Statistical significance was set at $p < 0.05$ (two-sided) for all analyses. The analyses were performed with SAS JMP Pro 16.1 (SAS Institute, Cary, NC).

3. Results

3.1. Demographics

The mean age of the study population at midlife in the year 2000 was 55.2 (range 50 to 65) years; 70.7 (range 66 to 80) years at the time of the late-life baseline [^{11}C]PIB-PET scans in 2014–2016; and 75.4 (range 70 to 86) years at the time of the late-life follow-up [^{11}C]PIB-PET scans in 2019–2021 (Table 1A). The mean follow-up time between the PET scans was 4.7 (SD 0.6) years. The IR+ group ($n = 19$) included 11 (57 %) *APOE*ε4 carriers and the IR− group ($n = 24$) included 11 (46 %) *APOE*ε4 carriers. There were no differences between IR− and IR+ groups on age, sex, *APOE*ε4 carriership status, time from midlife measurements to 20-year follow-up [^{11}C]PIB-PET scans or time between [^{11}C]PIB-PET scans (Table 1A). The IR+ group had higher HbA1c, serum total cholesterol, more often medication for type 2 diabetes and a lower level of education than IR− group (Table 1A).

The characteristics of the stratified IR/*APOE* groups are shown in Table 1B. The IR/*APOE* groups did not differ among age, sex, education, [^{11}C]PIB dose or CERAD total score at baseline in 2014–2016 (Table 1B). All 6 participants diagnosed with diabetes were receiving metformin medication and one of them was using combination of liraglutide and metformin in the IR+/ *APOE*ε4− group.

The group of individuals who participated in the baseline [^{11}C]PIB-PET study 2014–2016, but not in the follow-up in 2019–2021 ($n = 17$) did not differ from those who participated in both neuroimaging studies ($n = 43$) in terms of age ($p = 0.28$), CERAD total score ($p = 0.31$), or [^{11}C]PIB composite score at baseline in 2014–2016 ($p = 0.86$). In addition, the group in which the participant belonged to (IR/*APOE*) was not associated with taking part in the follow-up studies ($p = 0.24$). The persons who did not participate in the late-life follow-up study did not differ from those who participated in the 5-year follow-up in medication for type 2 diabetes ($p = 0.14$) or hypertension ($p = 0.96$) or other cardiovascular disease than hypertension ($p = 0.72$) at baseline.

3.2. Midlife IR and APOE genotype predicted higher [^{11}C]PIB composite SUVr after 20 years

[^{11}C]PIB composite SUVr at the late-life follow-up, 20 years after the measurement of midlife IR, was significantly higher in the IR+ group than in the IR− group ([^{11}C]PIB composite SUVr median 2.3 (interquartile range, IQR 1.7–3.3) vs. 1.7 (IQR 1.5–2.4), $p = 0.03$) (Fig. 2A, Table 2). *APOE* genotype was a strong predictor of [^{11}C]PIB composite SUVr at follow-up ($p < 0.0001$). IR group predicted [^{11}C]PIB composite SUVr at follow-up also after adjusting for *APOE* genotype ($p = 0.03$). The association between IR status and [^{11}C]PIB composite SUVr was borderline significant after further adjustments for age and sex ($p = 0.06$). IR group predicted [^{11}C]PIB composite SUVr at follow-up after adjusting for age, sex and education ($p = 0.01$). (Table 2).

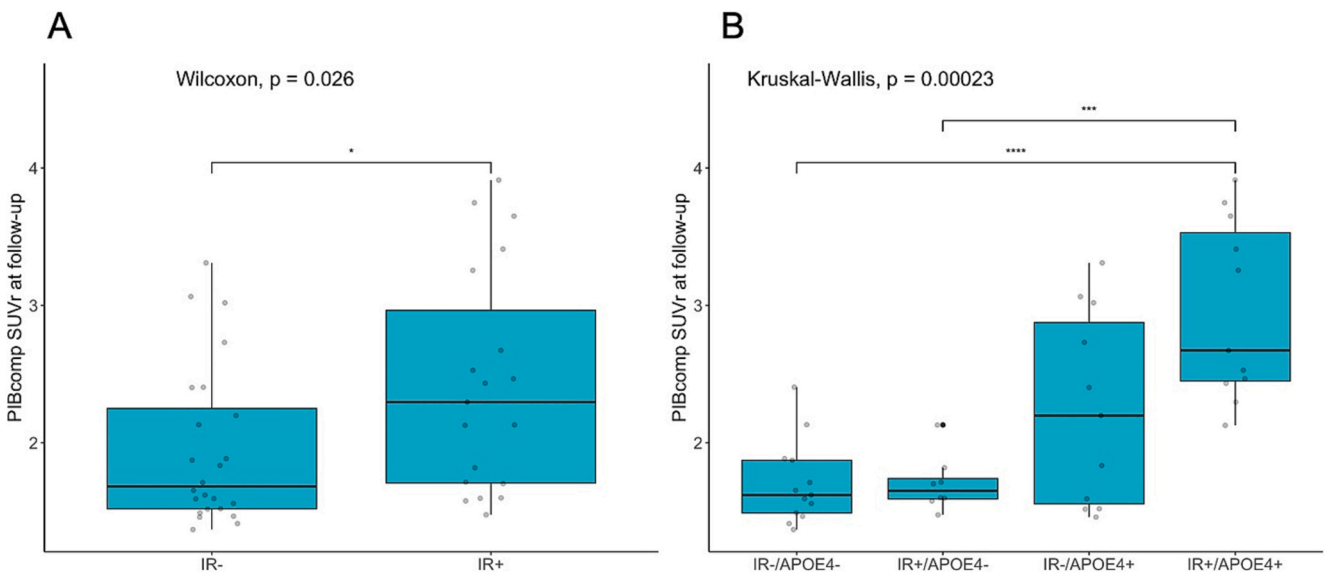

Fig. 2. [^{11}C]PIB composite SUVr at late-life follow-up according to (A) midlife insulin resistance (IR) group and (B) IR/*APOE* group.
The box plots show median [^{11}C]PIB composite standardized uptake value ratio (SUVr) values with interquartile ranges. Group differences are assessed with non-parametric tests. Pairwise comparisons among the insulin resistance and *APOE* genotype (IR/*APOE*) groups were evaluated with the Steel-Dwass method. *p*-values: * < 0.05; *** < 0.001; **** < 0.0001.

Table 2
Adjusted associations between insulin resistance (IR) group (IR− vs. IR+) and IR/*APOE* groups and [^{11}C]PIB composite standardized uptake value ratio (SUVr) at late-life follow-up.

	[^{11}C]PIB composite SUVr at late-life follow-up		
	β (SE)	95% confidence interval	*p* value
IR group	−0.24 (0.11)	1.98 to 2.4	0.03
IR group	−0.19 (0.08)	−0.36 to −0.02	0.03
APOE genotype	−0.42 (0.08)	−0.59 to −0.26	<0.0001
IR group	−0.17 (0.08)	−0.34 to 0.004	0.06
APOE genotype	−0.45 (0.08)	−0.62 to −0.28	<0.0001
Age	0.03 (0.02)	−0.02 to 0.08	0.22
Sex	0.11 (0.09)	−0.06 to 0.28	0.20
IR group	−0.29 (0.11)	−0.52 to −0.06	0.01
Age	0.02 (0.03)	−0.05 to 0.08	0.6
Sex	−0.007 (0.11)	−0.23 to 0.22	0.96
Education	0.05 (0.03)	−0.01 to 0.10	0.12
IR/APOE group			<0.0001[a]
Age	0.03 (0.02)	−0.02 to 0.07	0.30
Sex	0.08 (0.08)	−0.09 to 0.25	0.33

The results are derived from linear models and shown as estimates (β) with standard error (SE) and 95% confidence intervals for each variable in each model. First, the analyses were adjusted for *APOE* genotype and then further for age, sex and education. The analyses for IR/*APOE* genotype were adjusted for age and sex. [a] = The *p*-value is defined for overall group differences between the four IR/*APOE* groups (IR−/APOEε4−; IR+/APOEε4−; IR−/APOEε4+; IR+/APOEε4+).

There was a difference among the IR/*APOE* groups in [^{11}C]PIB SUVr at the late-life follow-up ($p = 0.0002$). Pair-wise analyses showed that [^{11}C]PIB SUVr at follow-up was higher in the IR+/*APOE*ε4+ group than in either the IR−/*APOE*ε4− ($p < 0.001$) or IR+/*APOE*ε4− groups ($p = 0.002$) (Fig. 2B). No significant differences were found among the other IR/*APOE*ε4 groups (Fig. 2B). Adjusting for age and sex did not change these results ($p < 0.0001$ for overall differences among groups). (Table 2)

3.3. Difference in 5-year change from baseline to follow-up [^{11}C]PIB composite SUVr according to midlife insulin resistance group and APOEε4 genotype

There was no difference between IR+ and IR− groups in the 5-year change in [^{11}C]PIB composite SUVr ($p = 0.29$) (Fig. 3). Adjusting for age and sex, or age, sex and time between scans or age, sex and education did not change these results. (Table 3).

Change in [^{11}C]PIB SUVr from baseline to follow-up was greater in the IR+/*APOE*ε4+ group than in the IR−/*APOE*ε4− (median change (IQR) 0.8 (0.60–1.0) vs. 0.28 (0.14–0.47), $p = 0.02$) or IR+/*APOE*ε4− groups (median change (IQR) SUVr 0.8 (0.60–1.0) vs. 0.24 (0.06–0.40), $p = 0.046$). There was no difference between the IR+/*APOE* ε4+ and IR−/*APOE* ε4+ groups ($p = 0.86$). (Fig. 3) Adjusting for age and sex, or age, sex and time between scans did not change these results (Table 3).

3.4. Interactions between IR group and APOEε4 genotype

There was an interaction for 'IR group × APOEε4 genotype' on the association with [^{11}C]PIB composite SUVr at follow-up ($p = 0.03$). The 'IR group × APOEε4 genotype' interaction for the change in [^{11}C]PIB composite SUVr during the 5-year follow-up was not significant ($p = 0.29$). However, according to our hypothesis, analyses stratified for APOE genotype were performed also for the change in [^{11}C]PIB composite SUVr during the 5-year follow-up.

3.5. Continuous midlife HOMA-IR and late-life baseline HOMA-IR correlated with [^{11}C]PIB composite score at late-life follow-up

To evaluate whether midlife or late-life IR would be associated with brain Aβ accumulation we explored the non-parametric correlations between continuous midlife (measured in the year 2000), late-life baseline (measured in 2014–2016) and late-life follow-up (measured in 2019–2021) HOMA-IR and late-life follow-up [^{11}C]PIB composite SUVr (Fig. 4). Midlife HOMA-IR (Spearman's correlation coefficient (r_S) = 0.39, $p = 0.01$) and HOMA-IR in late-life baseline ($r_S = 0.34$, $p = 0.03$) and the average of midlife HOMA-IR and late-life baseline HOMA-IR ($r_S = 0.40$, $p = 0.009$) correlated with [^{11}C]PIB composite SUVr at follow-up in 2019–2021. There was no cross-sectional association between HOMA-IR and [^{11}C]PIB composite SUVr at the late-life follow-up ($r_S =$

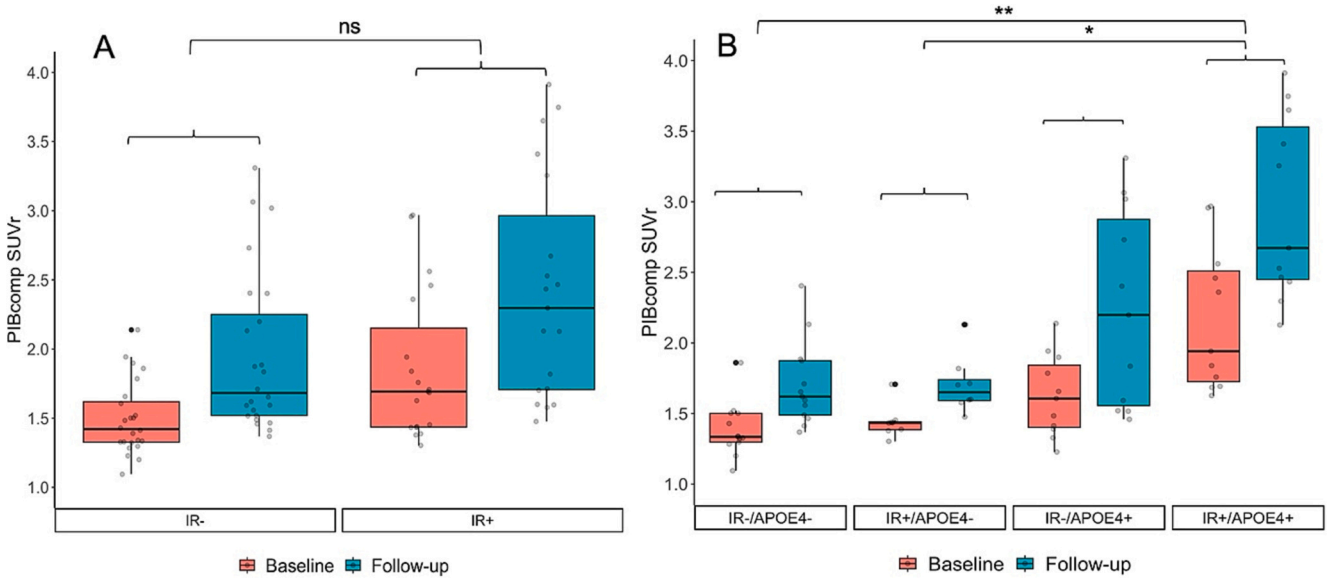

Fig. 3. 5-year change from baseline to follow-up in [^{11}C]PIB composite SUVr according to (A) midlife insulin resistance (IR) group and (B) IR/*APOE* group. The box plots show median [^{11}C]PIB composite SUVr values with interquartile ranges at late-life baseline and follow-up. Group differences are assessed with non-parametric Kruskall-Wallis test. Pairwise comparisons in the change from baseline to follow-up in [^{11}C]PIB composite SUVr among the IR/*APOE* groups were evaluated with the Steel-Dwass method. For Fig. 3B, only pairwise differences with *p*-values <0.05 are shown with star symbols. *p*-values: * < 0.05; ** < 0.01. Ns = non-significant.

Table 3
Adjusted associations between insulin resistance (IR) (IR− vs IR+) and IR/*APOE* groups and 5-year change in [^{11}C]PIB composite standardized uptake value ratio (SUVr).

	5-year change in [^{11}C]PIB composite SUVr		
	β (SE)	95% confidence interval	*p* value
IR group	−0.05 (0.06)	−0.18 to 0.08	0.42
Age	0.007 (0.02)	−0.03 to 0.04	0.71
Sex	0.01 (0.06)	−0.12 to 0.14	0.86
IR group	−0.05 (0.07)	−0.18 to 0.08	0.44
Age	0.007 (0.02)	−0.03 to 0.05	0.72
Sex	0.01 (0.07)	−0.12 to 0.14	0.88
Time between scans	−0.003 (0.11)	−0.22 to 0.22	0.98
IR group	−0.08 (0.06)	−0.22 to 0.05	0.20
Age	0.01 (0.02)	−0.03 to 0.05	0.59
Sex	−0.02 (0.06)	−0.15 to 0.11	0.79
Education	0.03 (0.02)	−0.006 to 0.06	0.10
IR/APOE group			0.003 [a]
Age	0.01 (0.02)	−0.02 to 0.05	0.45
Sex	0.03 (0.06)	−0.08 to 0.14	0.56
IR/APOE group			0.003[a]
Age	0.01 (0.02)	−0.02 to 0.05	0.43
Sex	0.05 (0.06)	−0.07 to 0.17	0.40
Time between scans	0.09 (0.10)	−0.11 to 0.28	0.37

The results are derived from linear models and shown as estimate (β) with standard error (SE) and 95% confidence intervals for each variable in each model. First, the analyses were adjusted for age and sex and then further for time between scans and education. The analyses for IR/*APOE* genotype were adjusted for age and sex, and then further for time between the [^{11}C]PIB-PET scans. [a] = The *p*-value is defined for overall group differences among the four IR/*APOE* groups (IR−/*APOEε4*−; IR+/*APOEε4*−; IR−/*APOEε4*+; IR+/*APOEε4*+).

0.24, $p = 0.13$).

3.6. Statistical parametric mapping (SPM) showing differences in the change of 5-year [^{11}C]PIB SUVr between the IR+/APOEε4+ and IR−/APOEε4- groups

The results of voxel-by-voxel differences (Fig. 5) showed that the change in [^{11}C]PIB SUVr from baseline to follow-up was greater in the IR+/ *APOEε4*+ group when compared to the IR−/ *APOEε4*- group in the right temporal cortex, and also in the frontal and parietal cortices as shown in Fig. 4.

4. Discussion

In community-dwelling, dementia-free elderly individuals, midlife IR did not predict a greater increase in Aβ accumulation during the five-year [^{11}C]PIB-PET imaging follow-up (from 15 to 20 years after midlife) in regions typical for Aβ accumulation in AD in the whole study group. Most importantly, individuals with both midlife IR and *APOEε4* allele had a greater increase in brain Aβ load during the 5-year follow-up when compared to *APOEε4* non-carriers with either normal midlife insulin sensitivity or midlife IR. This finding suggests that the presence of *APOEε4* might accelerate the rate of late-life brain Aβ accumulation individuals with midlife IR. In line with our previous findings, midlife IR predicted higher brain Aβ load 20 years later in late-life. We also found that both mid- and late-life HOMA-IR measured 20 and 5 years before the [^{11}C]PIB-PET scans was associated with Aβ accumulation. However, there was no cross-sectional association between HOMA-IR and Aβ load in late-life.

Our results are in line with previous studies suggesting that specifically midlife would be a crucial time phase for examining metabolic risk factors when evaluating their effect on cerebral Aβ accumulation (Ekblad et al., 2018; Gottesman et al., 2017; Willette et al., 2015; Hoscheidt et al., 2016). In contrast, late-life IR has not been associated with Aβ levels measured with PET (Pekkala et al., 2020; Laws et al., 2017) or from CSF (Laws et al., 2017; Ennis et al., 2021). In the present study continuous HOMA-IR was associated with cortical Aβ load when HOMA-IR was measured 20 or 5 years before the scans, but not cross-

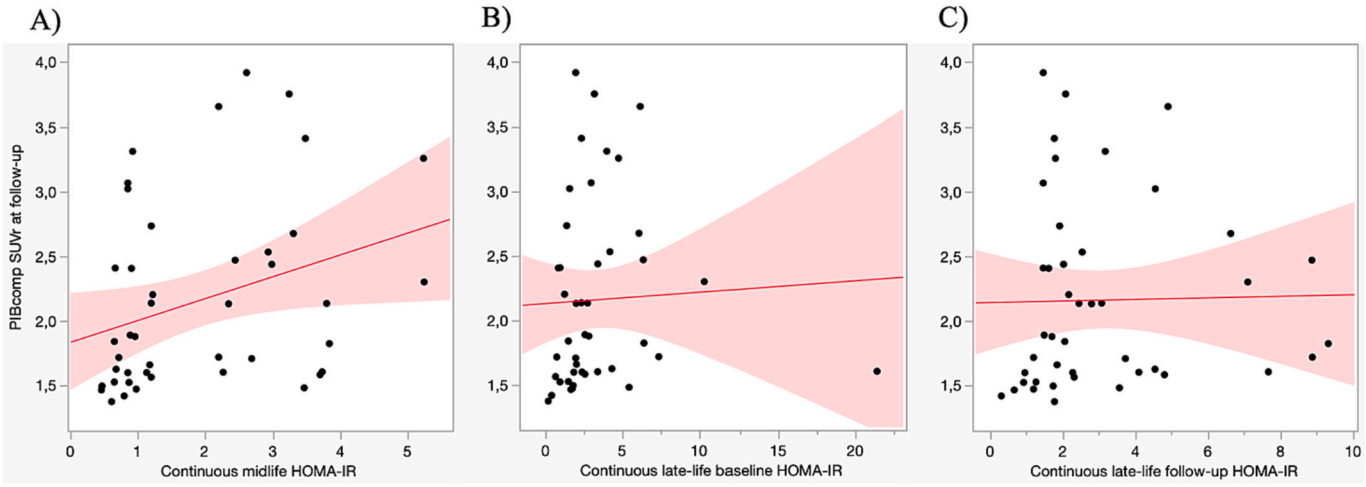

Fig. 4. Correlation between midlife HOMA-IR (A), late-life baseline HOMA-IR (B) and late-life follow-up HOMA-IR (C) and [^{11}C]PIB composite score at late-life follow-up.
The scatterplot matrixes with regression lines and 95% confidence intervals of the continuous association between HOMA-IR at different phases of the study and [^{11}C]PIB composite score at late-life follow-up.

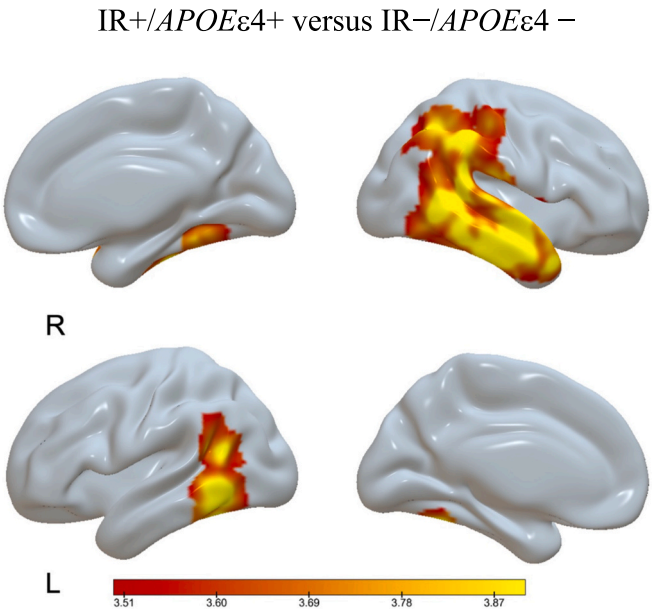

Fig. 5. Voxel-wise analyses for differences between IR+/*APOE*ε4+ and IR−/*APOE*ε4− groups in the change in [^{11}C]PIB composite SUVr during the 5-year follow-up.
Voxel-by-voxel analysis of the difference between the IR+/*APOE* ε4+ and IR−/*APOE* ε4− groups in the change of [^{11}C]PIB uptake during the 5-year follow-up, assessed with statistical parametric mapping (SPM). Change in [^{11}C]PIB uptake during the 5-year follow-up in the IR+/*APOE* ε4+ and IR−/*APOE* ε4− groups was first obtained by calculating the difference of normalized and smoothed follow-up and baseline [^{11}C]PIB SUVr images. Cortical regions where the difference between the groups was significant are shown in color in the image, yellow being most significant. Multiple comparisons were corrected using false discovery rate (FDR) by using a cluster-defining threshold of $p < 0.001$ and where the $p < 0.05$ FDR-corrected critical cluster size was 862 voxels. Right (R) and left (L) sides of the cortex are marked in the figure.

sectionally. Since Aβ accumulation is a slow process that begins approximately 20 years before the onset of cognitive decline, it is logical that risk factors for Aβ accumulation might be more important at the early phases of Aβ accumulation. Moreover, as an extension to previous findings, we found participants presenting with both *APOE*ε4 and IR to be at greatest risk for subsequent amyloid accumulation. Focusing on this interaction is clinically important, as individuals with metabolic risk factors and *APOE*ε4 have been found to benefit from multimodal intervetions, as indicated by FINGER study (Solomon et al., 2018). To date, there is some literature exploring this interaction. In the ARIC study the association between midlife obesity and late-life Aβ accumulation was found in *APOE*ε4 carriers, but not in non-carriers, although there was no statistically significant interaction for IR and *APOE* genotype (Gottesman et al., 2017).

Previous studies evaluating the association between IR and in vivo biomarkers of AD that would include repeated measurements are scarce. In a study with repeated CSF sampling from late midlife, IR was not related to the change in CSF biomarkers of AD in non-demented adults (Ennis et al., 2021). Secondary analyses indicated an interaction for *APOE*ε4 genotype, suggesting that higher IR predicted a higher CSF phospho-tau$_{181}$/Aβ$_{42}$ ratio in *APOE*ε4 carriers only (Ennis et al., 2021). The Baltimore Longitudinal Study of Aging study indicated that metabolic syndrome assessed at late-life was associated with a greater increase in Aβ accumulation in individuals who were Aβ positive at baseline (Gomez et al., 2018). Our findings extend the previous studies by providing measurements of HOMA-IR already in midlife; by enriching the study population for *APOE*ε4 carriers; by measuring brain Aβ accumulation in two late-life time points; and by extending the follow-up to 20 years from midlife.

Our finding in this longitudinal [^{11}C]PIB-PET imaging 5-year follow-up study revealed that midlife IR was not associated with the increased change in Aβ accumulation in late-life during ages from 70.7 to 75.4 years (mean), although the total Aβ burden was significantly greater in the IR group. However, in subgroup analyses, Aβ burden change in late-life was significantly higher in the group with IR and *APOE*ε4 genotype than in groups with normal insulin sensitivity and *APOE*ε4 non-carriers as well as in group with IR and *APOE*ε4 non-carriers. It is well known that Aβ accumulation begins at least 20 years before the onset of cognitive decline in the AD continuum (Rowe et al., 2010). Older age and especially *APOE*ε4 carrier status are associated with accelerated amyloid abnormality prevalence, and in late-life this curve is sharp (Jansen et al., 2022). Our results suggest that in addition to these previously established risk factors for Aβ accumulation, IR could also play an important role in the late-life Aβ accumulation rate in *APOE*ε4 carriers.

The mechanisms underlying the association between IR and Aβ has been widely studied in rodents and in in vitro models. It has been

demonstrated that insulin protects against Aβ synaptotoxicity and modulates its clearance from the brain (Zhao et al., 2009). Insulin and Aβ share a common degrading enzyme in the brain, and in IR this enzyme seems to be down-regulated which can result in increased Aβ accumulation (Pandini et al., 2013). Moreover, it has been shown that in human apoE-targeted replacement mice aged apoE4, but not apoE3 mice developed cerebral IR which was further exacerbated by a high-saturated fat diet and peripheral IR (Zhao et al., 2017).Recently, it was demonstrated that $A\beta_{40}$ monomers can bind to and activate insulin receptors, but that $A\beta_{40}$ oligomers can block insulin receptors, resulting in impaired insulin function (Molina-Fernández et al., 2022). Together, these preclinical studies imply that there could be a mechanistic link between IR and Aβ.

The strengths of our study are the long follow-up with repeated measurements of both IR and Aβ PET; the well-characterized study population; the measurement of midlife IR; and enriching the study population for *APOE*ε4 carriers. Amyloid accumulation was also determined with automatized Magia toolbox pipeline resulting a quantitative continuous scale of SUVr without cutoff points. However, there are also limitations: We did not measure tau pathology which has also been associated with IR, and which is known to correlate better with the clinical symptoms of AD, i.e. cognitive decline, than brain Aβ accumulation. However, our study population was still relatively well-preserved cognitively at follow-up and therefore we would not have expected our participants to have wide-spread tau pathology. Our study was relatively small which might limit firm conclusions that can be drawn from these data. According to previous test-re-test analyses and the power calculations of the present study, the study groups were large enough to detect a 15% difference in cortical Aβ. There were a few dropouts since the late-life baseline study. These individuals were mostly from the IR+/*APOE*ε4− group which might have diluted our results considering differences between the IR groups. We found no significant differences between the dropouts and the follow-up study population among medication for type 2 diabetes, hypertension, or other cardiovascular diseases than hypertension nor among strokes at the baseline. The individuals with midlife IR were more likely to be on diabetic medications than those who were insulin sensitive in midlife. Since diabetes medications often target insulin resistance, this difference would have diluted our results, rather than resulted in false positive association between IR and Aβ.

To conclude, we demonstrate that midlife IR predicts brain Aβ after a follow-up of 20 years, and that especially *APOE*ε4 carriers with midlife IR are at an increased risk for late-life Aβ accumulation and increased change in Aβ burden in late-life. These results together with the previous literature suggest that interventions targeted at reducing dementia risk might be most useful in *APOE*ε4 carriers with midlife insulin resistance.

Funding

This study project was funded by the Juho Vainio Foundation, the Sigrid Juselius Foundation and the Finnish Governmental Research Funding (VTR) for Turku University Hospital. EP was supported by the Finnish Governmental Research Funding (VTR) for Turku University Hospital, the Yrjö Jahnsson Foundation, the Betania Foundation, the Paulo Foundation, the Finnish Medical Foundation and the Uulo Arhio Memorial Foundation. LLE was supported by the Finnish Medical Foundation, the Emil Aaltonen Foundation, the Paulo Foundation and the Finnish Governmental Research Funding (VTR) for Turku University Hospital. AS holds a postdoctoral fellowship from the Research Council of Finland (#341059). JT was supported by the Finnish Governmental Research Funding (VTR) for Turku University Hospital. JOR has received funding from the Research Council of Finland (project #310962), the Sigrid Juselius Foundation and the Finnish Governmental Research Funding (VTR) for Turku University Hospital.

CRediT authorship contribution statement

Pietilä Elina: Conceptualization, Formal analysis, Funding acquisition, Methodology, Visualization, Writing – original draft, Writing – review & editing. **Snellman Anniina:** Writing – review & editing. **Tuisku Jouni:** Software, Visualization, Writing – review & editing. **Helin Semi:** Investigation, Writing – review & editing. **Viitanen Matti:** Conceptualization, Funding acquisition, Methodology, Supervision, Writing – review & editing. **Jula Antti:** Conceptualization, Methodology, Supervision, Writing – review & editing. **O. Rinne Juha:** Conceptualization, Funding acquisition, Methodology, Supervision, Writing – review & editing. **L. Ekblad Laura:** Conceptualization, Funding acquisition, Methodology, Project administration, Supervision, Visualization, Writing – original draft, Writing – review & editing.

Declaration of Competing Interest

None.

Data availability

Anonymized data may be shared according to a reasonable request by a qualified investigator who has a research plan with local ethical and institutional approval.

Acknowledgements

The participants of the studies are warmly acknowledged for their commitment to the studies. The authors would also like to acknowledge the staff of Turku PET Centre for their assistance during the study.

References

Aalto, S., Scheinin, N.M., Kemppainen, N.M., et al., 2009. Reproducibility of automated simplified voxel-based analysis of PET amyloid ligand [11C]PIB uptake using 30-min scanning data. Eur. J. Nucl. Med. Mol. Imaging 36 (10), 1651–1660. https://doi.org/10.1007/s00259-009-1174-1.

Chandler, M.J., Lacritz, L.H., Hynan, L.S., et al., 2005. A total score for the CERAD neuropsychological battery. Neurology. 65 (1), 102–106. https://doi.org/10.1212/01.wnl.0000167607.63000.38.

Ekblad, L.L., Rinne, J.O., Puukka, P., et al., 2017. Insulin resistance predicts cognitive decline: an 11-year follow-up of a nationally representative adult population sample. Diabetes Care 40 (6), 751–758. https://doi.org/10.2337/dc16-2001.

Chatterjee, S., Peters, S.A.E., Woodward, M., et al., 2016. Type 2diabetes as a risk factor for dementia in women compared with men: A pooled analysis of 2.3 million people comprising more than 100,000 cases of dementia. Diabetes Care 39 (2), 300–307. https://doi.org/10.2337/dc15-1588.

Ekblad, L.L., Johansson, J., Helin, S., et al., 2018. Midlife insulin resistance, APOE genotype, and late-life brain amyloid accumulation. Neurology. 90 (13) https://doi.org/10.1212/WNL.0000000000005214.

Ennis, G.E., Koscik, R.L., Ma, Y., et al., 2021. Insulin resistance is related to cognitive decline but not change in CSF biomarkers of Alzheimer's disease in non-demented adults. Alzheimers Dement. Diagn. Assess Dis. Monit. 13 (1) https://doi.org/10.1002/dad2.12220.

Gomez, G., Beason-Held, L.L., Bilgel, M., et al., 2018. Metabolic syndrome and amyloid accumulation in the aging brain. J. Alzheimers Dis. 65 (2), 629–639. https://doi.org/10.3233/JAD-180297.

Gottesman, R.F., Schneider, A.L.C., Zhou, Y., et al., 2017. Association between midlife vascular risk factors and estimated brain amyloid deposition. JAMA - J. Am. Med. Assoc. 317 (14), 1443–1450. https://doi.org/10.1001/jama.2017.3090.

Grothe, M.J., Barthel, H., Sepulcre, J., Dyrba, M., Sabri, O., Teipel, S.J., 2017. In vivo staging of regional amyloid deposition. Neurology. 89 (20), 2031–2038. https://doi.org/10.1212/WNL.0000000000004643.

Heistaro, S., 2008. Methodology Report: Health 2000 Survey. B26/2008. Finnish Institute for Health and Welfare.

Hoscheidt, S.M., Starks, E.J., Oh, J.M., et al., 2016. Insulin resistance is associated with increased levels of cerebrospinal fluid biomarkers of Alzheimer's disease and reduced memory function in at-risk healthy middle-aged adults. J. Alzheimers Dis. 52 (4), 1373–1383. https://doi.org/10.3233/JAD-160110.

Jänis, M.T., Siggins, S., Tahvanainen, E., et al., 2004. Active and low-active forms of serum phospholipid transfer protein in a normal Finnish population sample. J. Lipid Res. 45 (12), 2303–2309. https://doi.org/10.1194/jlr.M400250-JLR200.

Jansen, W.J., Janssen, O., Tijms, B.M., et al., 2022. Prevalence estimates of amyloid abnormality across the Alzheimer disease clinical Spectrum. JAMA Neurol. 79 (3), 228–243. https://doi.org/10.1001/jamaneurol.2021.5216.

Karjalainen, T., Tuisku, J., Santavirta, S., et al., 2020. Magia: robust automated image processing and kinetic modeling toolbox for PET neuroinformatics. Front. Neuroinform. 14, 3. https://doi.org/10.3389/fninf.2020.00003.

Kim, A.B., Arvanitakis, Z., 2023. Insulin resistance, cognition, and Alzheimer disease. Obesity. 31 (6), 1486–1498. https://doi.org/10.1002/oby.23761.

Kivipelto, M., Ngandu, T., Fratiglioni, L., et al., 2005. Obesity and Vascular Risk Factors at Midlife and the Risk of Dementia and Alzheimer Disease. Arch Neurol. 2005;62 (10), 1556–1560. https://doi.org/10.1001/archneur.62.10.1556.

Laws, S.M., Gaskin, S., Woodfield, A., et al., 2017. Insulin resistance is associated with reductions in specific cognitive domains and increases in CSF tau in cognitively normal adults. Sci. Rep. 7 (1) https://doi.org/10.1038/s41598-017-09577-4.

Leclerc, M., Bourassa, P., Tremblay, C., et al., 2022. Cerebrovascular insulin receptors are defective in Alzheimer's disease. Brain. https://doi.org/10.1093/brain/awac309. Published online October 25.

Lopresti, B.J., Klunk, W.E., Mathis, C.A., et al., 2005. Simplified quantification of Pittsburgh compound B amyloid imaging PET studies: a comparative analysis. J. Nucl. Med. 46 (12), 1959–1972.

Lumsden, A.L., Mulugeta, A., Zhou, A., Hyppönen, E., 2020. Apolipoprotein E (APOE) genotype-associated disease risks: a phenome-wide, registry-based, case-control study utilising the UK Biobank. EBioMedicine. 59, 102954 https://doi.org/10.1016/j.ebiom.2020.102954.

Matthews, D.R., Hosker, J.P., Rudenski, A.S., Naylor, B.A., Treacher, D.F., Turner, R.C., 1985. Homeostasis model assessment: insulin resistance and beta-cell function from fasting plasma glucose and insulin concentrations in man. Diabetologia. 28 (7), 412–419. https://doi.org/10.1007/BF00280883.

Molina-Fernández, R., Picón-Pagès, P., Barranco-Almohalla, A., et al., 2022. Differential regulation of insulin signaling by monomeric and oligomeric amyloid beta-peptide. Brain Commun. https://doi.org/10.1093/braincomms/fcac243. Published online September 1.

Morris, J.C., Heyman, A., Mohs, R.C., et al., 1989. The consortium to establish a registry for Alzheimer's disease (CERAD). Part I. Clinical and neuropsychological assessment of Alzheimer's disease. Neurology. 39 (9), 1159–1165. https://doi.org/10.1212/wnl.39.9.1159.

Pandini, G., Pace, V., Copani, A., Squatrito, S., Milardi, D., Vigneri, R., 2013. Insulin has multiple antiamyloidogenic effects on human neuronal cells. Endocrinology. 154 (1), 375–387. https://doi.org/10.1210/en.2012-1661.

Peila, R., Rodriguez, B.L., Launer, L.J., Honolulu-Asia Aging Study, 2002. Type 2 diabetes, APOE gene, and the risk for dementia and related pathologies: the Honolulu-Asia aging study. Diabetes. 51 (4), 1256–1262. https://doi.org/10.2337/diabetes.51.4.1256.

Pekkala, T., Hall, A., Mangialasche, F., et al., 2020. Association of peripheral insulin resistance and other markers of type 2 diabetes mellitus with brain amyloid deposition in healthy individuals at risk of dementia. J. Alzheimers Dis. 76 (4), 1243–1248. https://doi.org/10.3233/JAD-200145.

Rowe, C.C., Ellis, K.A., Rimajova, M., et al., 2010. Amyloid imaging results from the Australian Imaging, Biomarkers and Lifestyle (AIBL) study of aging. Neurobiol. Aging 31 (8), 1275–1283. https://doi.org/10.1016/j.neurobiolaging.2010.04.007.

Shieh, J.C.C., Huang, P.T., Lin, Y.F., 2020. Alzheimer's disease and diabetes: insulin signaling as the bridge linking two pathologies. Mol. Neurobiol. 57 (4), 1966–1977. https://doi.org/10.1007/s12035-019-01858-5.

Snellman, A., Rokka, J., López-Picón, F.R., et al., 2017. Applicability of [(11)C]PIB micro-PET imaging for in vivo follow-up of anti-amyloid treatment effects in APP23 mouse model. Neurobiol. Aging 57, 84–94. https://doi.org/10.1016/j.neurobiolaging.2017.05.008.

Solomon, A., Turunen, H., Ngandu, T., et al., 2018. Effect of the apolipoprotein e genotype on cognitive change during a multidomain lifestyle intervention a subgroup analysis of a randomized clinical trial. JAMA Neurol. 75 (4), 462–470. https://doi.org/10.1001/jamaneurol.2017.4365.

Talbot, K., Wang, H.Y., Kazi, H., et al., 2012. Demonstrated brain insulin resistance in Alzheimer's disease patients is associated with IGF-1 resistance, IRS-1 dysregulation, and cognitive decline. J. Clin. Invest. 122 (4), 1316–1338. https://doi.org/10.1172/JCI59903.

Tang, X., Zhao, W., Lu, M., et al., 2021. Relationship between central obesity and the incidence of cognitive impairment and dementia from cohort studies involving 5,060,687 participants. Neurosci. Biobehav. Rev. 130, 301–313. https://doi.org/10.1016/j.neubiorev.2021.08.028.

Thambisetty, M., Metter, E.J., Yang, A., et al., 2013. Glucose intolerance, insulin resistance, and pathological features of Alzheimer disease in the Baltimore longitudinal study of aging. JAMA Neurol. 70 (9), 1167–1172. https://doi.org/10.1001/jamaneurol.2013.284.

Toppala, S., Ekblad, L.L., Lötjönen, J., et al., 2019. Midlife insulin resistance as a predictor for late-life cognitive function and cerebrovascular lesions. J. Alzheimers Dis. 72 (1) https://doi.org/10.3233/JAD-190691.

Toppala, S., Ekblad, L.L., Tuisku, J., et al., 2021. Association of early β-amyloid accumulation and neuroinflammation measured with [(11)C]PBR28 in elderly individuals without dementia. Neurology. 96 (12), e1608–e1619. https://doi.org/10.1212/WNL.0000000000011612.

van Arendonk, J., Neitzel, J., Steketee, R.M.E., et al., 2023. Diabetes and hypertension are related to amyloid-beta burden in the population-based Rotterdam Study. Brain. 146 (1), 337–348. https://doi.org/10.1093/brain/awac354.

Vemuri, P., Schöll, M., 2017. Linking amyloid-β and tau deposition in Alzheimer disease. JAMA Neurol. 74 (7), 766–768. https://doi.org/10.1001/jamaneurol.2017.0323.

Willette, A.A., Johnson, S.C., Birdsill, A.C., et al., 2015. Insulin resistance predicts brain amyloid deposition in late middle-aged adults. Alzheimers Dement. J. Alzheimers Assoc. 11 (5), 504–510.e1. https://doi.org/10.1016/j.jalz.2014.03.011.

Zhao, W.Q., Lacor, P.N., Chen, H., et al., 2009. Insulin receptor dysfunction impairs cellular clearance of neurotoxic oligomeric a{beta}. J. Biol. Chem. 284 (28), 18742–18753. https://doi.org/10.1074/jbc.M109.011015.

Zhao, N., Liu, C.C., Van Ingelgom, A.J., et al., 2017. Apolipoprotein E4 impairs neuronal insulin signaling by trapping insulin receptor in the endosomes. Neuron. 96 (1), 115–129.e5. https://doi.org/10.1016/j.neuron.2017.09.003.